Chemical Science

ROYAL SOCIETY OF CHEMISTRY

EDGE ARTICLE

View Article Online
View Journal | View Issue

Cite this: *Chem. Sci.*, 2024, **15**, 16307

All publication charges for this article have been paid for by the Royal Society of Chemistry

Enhancing the antibacterial efficacy of vancomycin analogues: targeting metallo-β-lactamases and cell wall biosynthesis†

Paramita Sarkar,[a] Weipan Xu,[b] Melissa Vázquez-Hernández,[c] Geetika Dhanda,[a] Shubhandra Tripathi,[d] Debajyoti Basak,[a] Hexin Xie,[b] Lea Schipp,[c] Pascal Dietze,[c] Julia E. Bandow,[c] Nishanth N. Nair[d] and Jayanta Haldar*[ae]

Vancomycin is a crucial last-resort antibiotic for tackling Gram-positive bacterial infections. However, its potency fails against the more difficult-to-treat Gram-negative bacteria (GNB). Vancomycin derivatives have shown promise as broad-spectrum antibacterials, but are still underexplored. Toward this, we present a novel strategy wherein we substitute the sugar moiety of vancomycin with a dipicolyl amine group, yielding VanNHdipi. This novel glycopeptide enhances its efficacy against vancomycin-resistant bacteria by up to 100-fold. A comprehensive approach involving microbiological assays, biochemical analyses, proteomics, and computational studies unraveled the impact of this design on biological activity. Our investigations reveal that VanNHdipi, like vancomycin, disrupts membrane-bound steps of cell wall synthesis inducing envelope stress, while also interfering with the structural integrity of the cytoplasmic membrane, setting it apart from vancomycin. Most noteworthy is its potency against critical GNB producing metallo-β-lactamases (MBLs). VanNHdipi effectively inactivates various MBLs with IC_{50} in the range of 0.2–10 μM resulting in resensitization of MBL-producing bacteria to carbapenems. Molecular docking and molecular dynamics (MD) studies indicate that H-bonding interactions between the sugar moiety of the vancomycin derivative with the amino acids on the surface of NDM-1 facilitate enhanced binding affinity for the enzyme. This work expands the scope of vancomycin derivatives and offers a promising new avenue for combating antibiotic resistance.

Received 31st May 2024
Accepted 8th September 2024

DOI: 10.1039/d4sc03577a

rsc.li/chemical-science

Introduction

The emergence of antibiotic resistance in both Gram-positive and Gram-negative bacteria (GPB and GNB respectively) has become a major concern to global health. In particular, the rise of vancomycin-resistant Gram-positive and carbapenem-resistant Gram-negative superbugs has emerged as a dire threat, exacerbated by the scarcity of treatment options.[1] Reports of carbapenem resistance are increasingly common among Gram-negative pathogens like *Escherichia coli* and *Klebsiella pneumoniae*.[2] The prevalence of multidrug resistance necessitates the development of novel antibiotics with unique mechanisms of action. This concern is highlighted in the joint ECDC-EMEA report, which emphasizes the scarcity of new antibiotics with novel mechanisms, especially for combating GNB.[3] One potential solution to this problem is the exploration of novel semi-synthetic antibiotics.

Vancomycin, a glycopeptide antibiotic, is a crucial last-resort drug used to treat Gram-positive bacterial infections. It acts by binding to the D-Ala-D-Ala moieties of the cell wall precursors, thereby inhibiting the final stage of bacterial cell wall synthesis. However, in vancomycin-resistant bacteria, a 1000-fold reduction in binding affinity to the mutated target, D-Ala-D-Lac, results in the loss of its effectiveness.[4] The second-generation glycopeptide antibiotics, dalbavancin, telavancin, and oritavancin use hydrophobic modifications on the vancosamine sugars to overcome resistance. Albeit, their efficacy varies depending on the strain and the type of vancomycin-resistance acquired by the corresponding bacteria.[5–7] Given their success, the development of semi-synthetic glycopeptides has been

[a]*Antimicrobial Research Laboratory, New Chemistry Unit, Jawaharlal Nehru Centre for Advanced Scientific Research, Jakkur, Bengaluru 560064, Karnataka, India. E-mail: jayanta@jncasr.ac.in; Tel: +91 802208 2565*

[b]*School of Pharmacy, East China University of Science and Technology, 130 Meilong Rd., Shanghai 200237, China*

[c]*Applied Microbiology, Faculty of Biology and Biotechnology, Ruhr University Bochum, Universitätsstraße 150, 44780 Bochum, Germany*

[d]*Department of Chemistry, Indian Institute of Technology Kanpur, Kanpur 20816, India*

[e]*School of Advanced Materials, Jawaharlal Nehru Centre for Advanced Scientific Research, Jakkur, Bengaluru 560064, Karnataka, India*

† Electronic supplementary information (ESI) available: supplementary figures; materials; experimental methods for *in vitro* microbiological assays (antibacterial activity, biofilms, time-kill kinetics, proteomics and mechanistic studies) and toxicity, and *in vivo* activity and toxicity; characterization of intermediates and final compounds through (^{1}HNMR, and HR-MS). See DOI: https://doi.org/10.1039/d4sc03577a

a propitious approach toward antibacterial drug discovery.[8] Some of the successful strategies that have been reported to overcome vancomycin resistance in GPB involve incorporating membrane disruptive moieties;[9–13] the enhancement of binding affinity to the target peptide or other components of the bacterial membrane;[14–16] and backbone modifications to substitute the lost binding affinity to the target.[17–19] These glycopeptide antibiotics are however not active against GNB due to the outer membrane, which serves as a barrier to their entry. Although reports of glycopeptide derivatives with activity against GPB and GNB are limited, there remains significant potential for their further development against a broader spectrum of pathogens.[20–24] The antibacterial activity and mechanisms of action of glycopeptide antibiotics pivot on the sites of functionalization of the glycopeptides.[4,22] An understanding of how these modifications affect activity is still limited. This gap necessitates further research and refinement to better understand how chemical modifications impact antibacterial activity.

We have reported multifunctional vancomycin derivatives that exhibit activity against both multidrug-resistant GPB and GNB.[22,25,26] We showed that the conjugation of cationic lipophilic moieties at the C-terminus of vancomycin results in activity against both types of bacteria. In contrast, the conjugation of cationic lipophilic moieties at the vancosamine sugar resulted in high antibacterial activity against the GPB but not against GNB.[27] In another strategy, we showed that the conjugation of a Zn(II) chelating ligand, dipicolyl-1,6-hexadiamine to the C-terminus of vancomycin resulted in Dipi-Van (**1**, Fig. 1A), which demonstrated a 375-fold enhancement in activity against vancomycin-resistant Enterococci (VRE).[14] The ability of the compound to form a Dipi-Van-Zn^{2+} complex with the pyrophosphate of lipid II on the outer surface of the bacterial membrane underpins its enhanced activity against VRE.[14] Notably, it inhibits the metallo-β-lactamase NDM-1, re-sensitizing NDM-producing bacteria to meropenem, as demonstrated in both *in vitro* and *in vivo* experiments.[28] The promising efficacy of Dipi-Van (**1**) called for further exploration and understanding of this design strategy to achieve even higher antibacterial activity against both GPB and GNB.

In this study, we present the development of a next-generation vancomycin-dipicolyl amine conjugate, VanNHdipi (**2**, Fig. 1A). Unlike Dipi-Van, herein, the dipicolyl amine moiety was conjugated at the primary amine of the vancosamine sugar of vancomycin to yield, VanNHdipi (**2**) using the synthetic protocol shown in Scheme S1.† We explore the antibacterial attributes of VanNHdipi, elucidating its efficacy against multidrug-resistant GPB and their biofilms. Additionally, its efficacy against a wide range of MBLs, for which effective inhibitors are scarce, was established. We compare its activity with Dipi-Van (**1**) and demonstrate the enhanced antibacterial efficacy of VanNHdipi (**2**). Through a combination of biochemical assays, proteomics and computational analyses, we investigate the mechanisms of action that underlie its

(A)

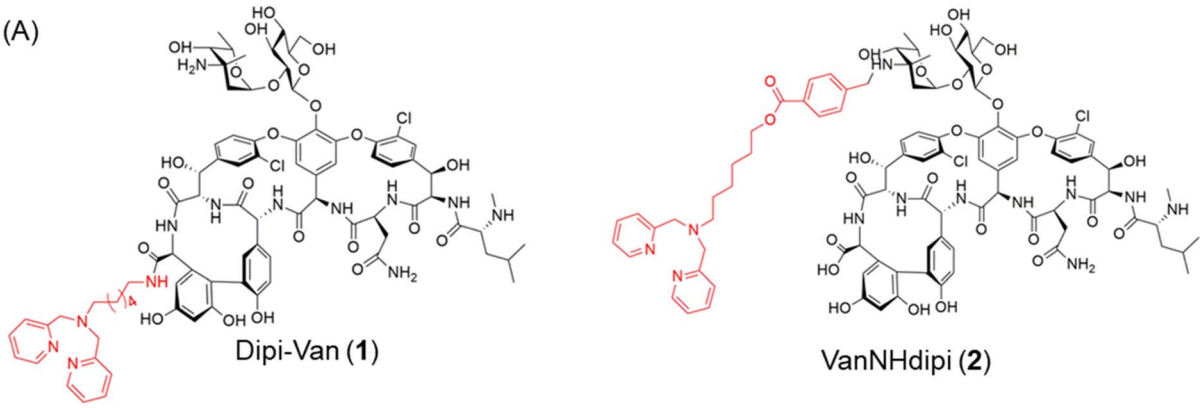

(B)

Compounds	MIC (μM)							
	MRSA	VRSA 1	VRSA 4	VRSA 12	VRE 903	VRE 909	VRE 51575	VRE 51559
Vancomycin	0.6	346	346	346	694	346	346	1388
Dipi-Van	1.7	27.9	7	27.9	27.9	27.9	1.5[a]	2[a]
VanNHdipi	0.8	6.6	3.3	1.6	6.6	13.2	6.6	13.2

Fig. 1 Structure and antibacterial activity of dipicolylamine functionalized vancomycin derivatives. (A) Vancomycin was functionalized at the C-terminus and the vancosamine nitrogen to yield Dipi-Van and VanNHdipi respectively, (B) MIC of vancomycin, Dipi-Van and VanNHdipi against various vancomycin-sensitive and resistant strains. MRSA, methicillin-resistant *S. aureus* (ATCC 33591); VRSA, vancomycin-resistant *S. aureus*; VRE vancomycin-resistant *E. faecium* (VanA phenotype, ATCC 51559); vancomycin-resistant *E. faecalis* (VanB phenotype, ATCC 51575); VRE 909 and 903 are vancomycin-resistant *E. faecium*. [a]Activity of Dipi-Van against VRE 51575 and VRE 51559 has been reported previously.[14]

antibacterial activity. This study emphasizes the importance of positional modification to augment the antibacterial properties of vancomycin.

Results and discussion

Vancosamine-functionalized derivative displays potent activity against Gram-positive bacteria

Antibacterial activity. The antibacterial activity of Dipi-Van (**1**) and VanNHdipi (**2**) was examined against various vancomycin-resistant strains of Staphylococci (VRSA) and Enterococci (VRE) (Fig. 1B). The minimum inhibitory concentration (MIC) values for vancomycin exceeded 346 μM (512 μg mL^{-1}) against all vancomycin-resistant strains (VRSA and VRE). Dipi-Van exhibited a MIC in the range of 1.5–28 μM, and VanNHdipi displayed improved activity with MICs ranging from 1.6–13.2 μM among strains. Compared to Dipi-Van, VanNHdipi displayed a 2 to 16-fold enhancement in antibacterial activity against six of the eight strains of VRSA and VRE tested. Further, the activity of VanNHdipi (MIC = 0.8 μM) against MRSA was at par with vancomycin (MIC = 0.6 μM).

***In vitro* toxicity.** Next, we tested the toxicity of VanNHdipi against mammalian cells (HEK cells) as the CC_{50} (50% cytotoxic concentration) and human red blood cells (RBCs) as the hemolytic activity, HC_{50} (50% hemolytic concentration), respectively. VanNHdipi did not exhibit any hemolytic activity against hRBCs up to 500 μM demonstrating the potential for a suitable therapeutic window (Fig. S1†). Additionally, the CC_{50} of the compound against the HEK cells was >80 μM. This indicated no toxicity at the concentrations required for antibacterial activity and supported the potential for further testing VanNHdipi as a preclinical candidate.

Kinetics of bactericidal activity. The kinetics of bactericidal activity upon treatment with VanNHdipi (**2**) was compared with that of vancomycin, against the vancomycin-sensitive MRSA. VanNHdipi (**2**) resulted in more rapid bactericidal activity than vancomycin (Fig. 2A). Vancomycin's bactericidal activity remains the same across concentrations and required 24 h for complete eradication. However, VanNHdipi (**2**) shows a time and concentration-dependent bactericidal activity. Within 6 h of treatment at MIC and higher concentrations, VanNHdipi (**2**) reduced bacterial counts by 1 to 1.2 Log CFU mL^{-1} (Fig. 2A). Upon treatment at MIC, it reduced the bacterial counts by 2.4 Log CFU mL^{-1} in 12 h and showed complete eradication at 24 h. At 2 × MIC and 4 × MIC, VanNHdipi (**2**) showed complete eradication in 12 h (5.4 Log CFU mL^{-1} reduction). This shows the improved antibacterial properties of VanNHdipi over vancomycin.

Eradicating MRSA biofilms. Biofilms, robust communities of bacteria enmeshed in a protective matrix, pose a formidable challenge in combating infections. Metal chelators like EDTA are known to eradicate biofilms, disperse bacteria, and reduce the viability of cells within these structures.[29,30] It was hypothesized that the presence of the metal chelating dipicolyl amine moiety, in both Dipi-Van (**1**) and VanNHdipi (**2**), could result in improved efficacy against MRSA biofilms. While vancomycin is active against exponential phase bacteria, it showed minimal activity against the biofilm (Fig. 2B). Treatment with Dipi-Van (**1**) and VanNHdipi (**2**) at 20 μM, resulted in a 1.3 Log CFU mL^{-1} and 2 Log CFU mL^{-1} reduction in cell viability within the biofilms respectively (Fig. 2B and C). Employing confocal microscopy, we observed that treatment with VanNHdipi for 24 h led to ∼60% reduction in biofilm thickness when compared to untreated control biofilms (Fig. 2C). Specifically, the thickness of these biofilms diminished from 14.5 μm in the untreated control to 8.3 μm following VanNHdipi treatment. VanNHdipi therefore also improved in activity against the more difficult to treat biofilms when compared to vancomycin and Dipi-Van.

Assessing *in vivo* efficacy against MRSA in a mouse thigh infection model. To evaluate the therapeutic potential of VanNHdipi (**2**) against MRSA *in vivo*, we conducted experiments using a neutropenic mouse thigh infection model. In this model, MRSA infection was induced by inoculating mice with $\sim 5 \times 10^5$ CFU of MRSA in the thigh. Subsequently, the mice were then treated with 12 mg kg^{-1} doses of vancomycin and VanNHdipi (**2**) intraperitoneally, with the initial dose administered 1 h post-infection, followed by a subsequent dose 13 h later (Fig. 2D). The mice were sacrificed 24 h post-infection. The pre-treatment bacterial load was 5.6 Log CFU g^{-1}. In the untreated control group, the bacterial load increased to 6.6 Log CFU g^{-1}. The vancomycin-treated group showed a bacterial load of 4.8 Log CFU g^{-1} of tissue. Treatment with VanNHdipi (**2**) yielded a significantly reduced bacterial load of 4.4 Log CFU g^{-1}, highlighting its efficacy in an *in vivo* setting.

VanNHdipi acts against Gram-positive bacteria through multiple modes of action

Antagonization in the presence of competing ligand *N*,*N*′-diacetyl–L-Lys–D-Ala–D-Ala. VanNHdipi showed much improvement in antibacterial efficacy compared to the parent drug vancomycin. We next investigated the mechanisms of action of our lead compound to understand what contributes to this improved activity. The parent drug vancomycin acts by binding to the D-Ala-D-Ala moiety of cell wall biosynthesis precursors. Therefore, competition assays using the D-alanine–D-alanine analog *N*,*N*′-diacetyl–L-Lys–D-Ala–D-Ala (KAA) were performed with vancomycin and VanNHdipi (**2**) to explore the dependence of antibiotic activity on interactions with the known binding site of vancomycin. The two compounds, vancomycin and VanNHdipi (**2**), were pre-incubated with KAA and then added to the bacterial solution for MIC determination. The MIC of vancomycin against MRSA increased from 0.6 μM to >30 μM in the presence of 500 μM of KAA, indicating that additional KAA, to a measurable extent, competes with target binding. The activity of VanNHdipi (**2**), however, was antagonized only 2-fold in the presence of 500 μM of KAA and not at all at the lower concentration of 250 μM (ESI S3†). This indicates that KAA does not compete as effectively with VanNHdipi (**2**) target binding. This could be because VanNHdipi (**2**) has a higher affinity for the vancomycin binding site than vancomycin, or that the antibacterial effect of VanNHdipi (**2**) only partially relies on the interaction with the known vancomycin target and the binding of additional targets are largely responsible for the activity.

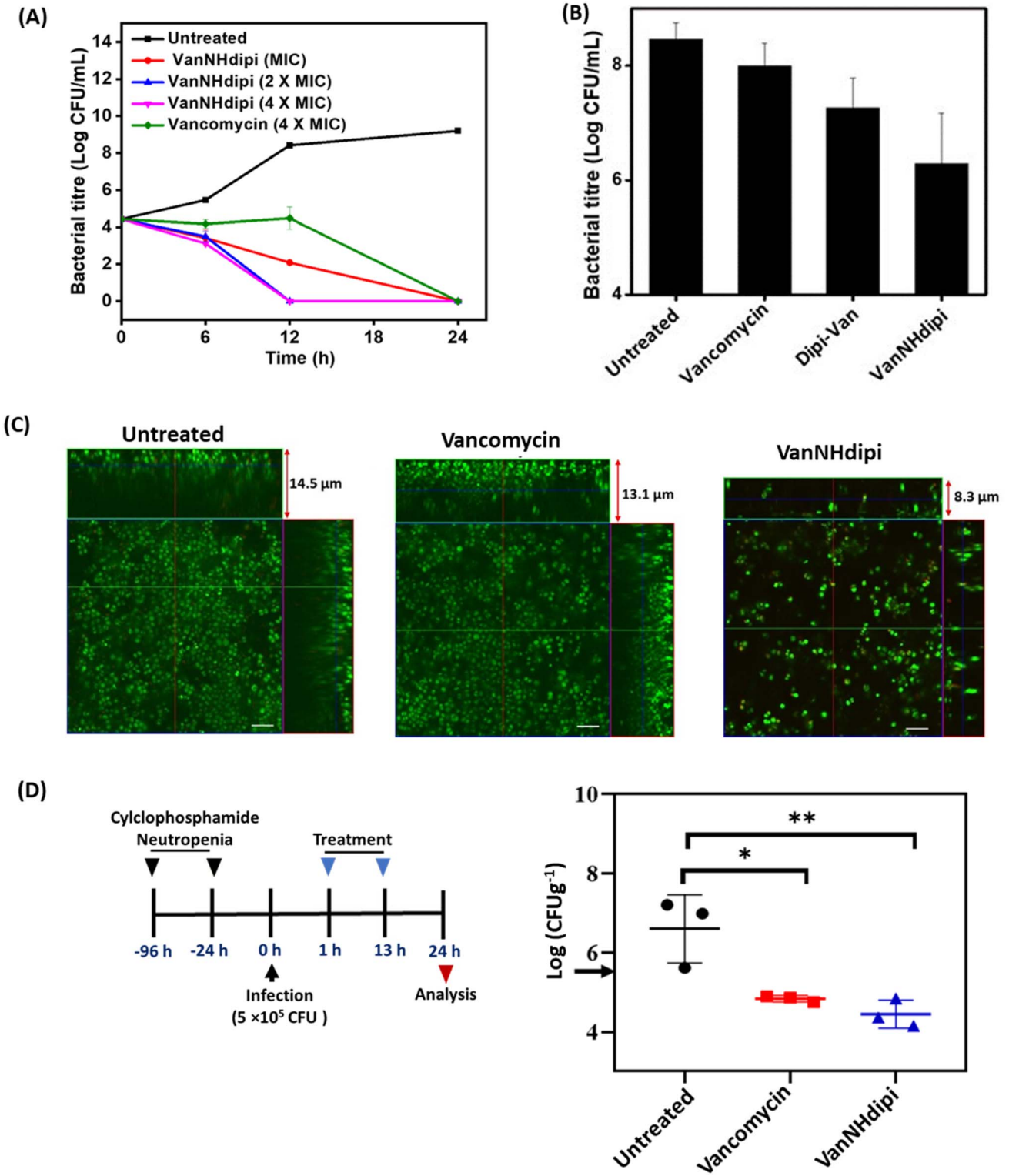

Fig. 2 Efficacy of VanNHdipi (**2**) against methicillin-resistant *S. aureus* (MRSA) in exponential phase, biofilms and a mouse thigh infection model. (A) Kinetics of bactericidal activity of VanNHdipi (**2**) and vancomycin against exponential growth phase MRSA. '*' indicates <50 CFU mL; (B) viability of cells within biofilms when treated with vancomycin and VanNHdipi at 20 μM; (C) confocal laser scanning microscopy when mature biofilms were left untreated, treated with vancomycin and VanNHdipi at 20 μM each; (scale bar = 5 μm); (D) *in vivo* efficacy of VanNHdipi and vancomycin against MRSA (n = 3/dose). Antibiotics were administered intraperitoneally twice at 12 h intervals at 12 mg kg^{-1} (left). Black arrow indicates pre-treatment bacterial load (right). Statistical analysis was done using One-way ANOVA. '*' indicates $p = 0.017$, '**' $p = 0.006$.

Acute effect on growth of *Bacillus subtilis* in mid-log phase. *B. subtilis* is a well-established Gram-positive model bacterium frequently employed to study the mechanism of action of compounds. Therefore, we next performed further mechanistic studies on this bacterium. The MIC of VanNHdipi (**2**) and vancomycin against *B. subtilis* were found to be 0.2 μM. To gain a deeper understanding of the mechanism of action of the compound, it was crucial to expose bacterial cells to concentrations at which growth could continue, albeit at reduced rate and with induction of a stress response.[31] We refer to this specific concentration as the physiologically effective concentration (PEC). To identify the PEC, first the bacteria were allowed to grow to an OD_{500} of 0.35 (mid-log phase) and then treated with different concentrations of a compound to observe its acute impact on bacterial growth (Fig. 3A). Notably, while vancomycin showed growth retardation only at 2 × MIC (0.4 μM), VanNHdipi (**2**) impeded bacterial growth even at lower concentrations, corresponding to 0.75 × MIC (0.16 μM) (Fig. S2†). At a higher concentration of 1.5 × MIC, a decrease in OD was observed potentially indicating cell lysis induced by VanNHdipi.

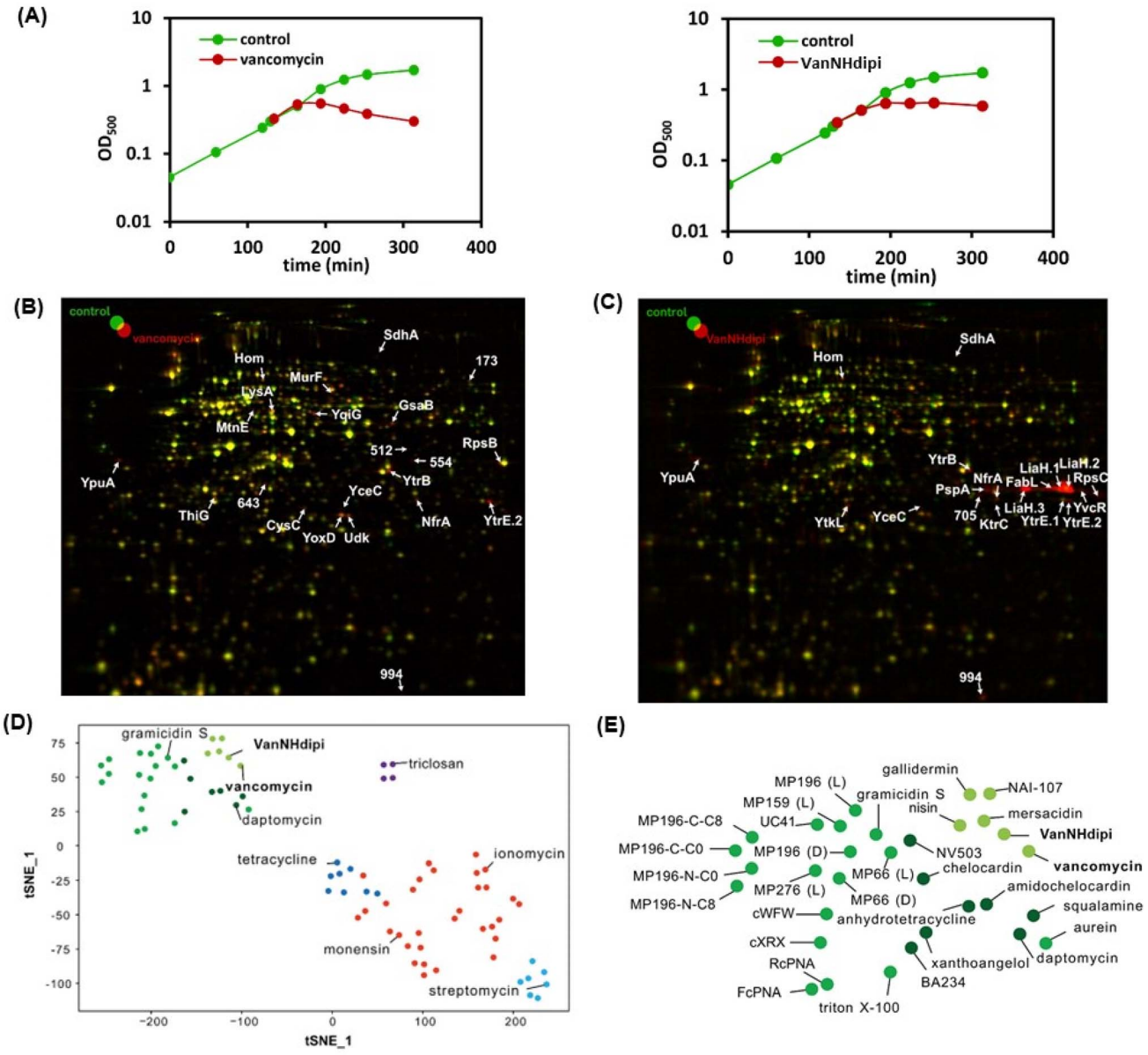

Fig. 3 (A) Acute growth retardation upon treatment of cultures of *B. subtilis* 168 with vancomycin at 0.4 μM (2 × MIC) and VanNHdipi 0.16 μM (0.75 × MIC) upon treatment at the PEC; 2D gel-based proteome analysis of vancomycin-treated *B. subtilis*. Synthesis of cytosolic proteins of (B) vancomycin-treated (false-colored in red), (C) VanNHdipi-treated (false-colored in red), and untreated (false-colored in green) *B. subtilis* were compared based on [^{35}S]-methionine labeling. In the overlaid autoradiographs, down-regulated proteins appear green, up-regulated proteins appear red, and proteins expressed at equal rates appear yellow. (D & E) The tSNE analysis serves to compare the similarity of proteome responses to a library of responses. (E) Details the upper left corner of (D). The response to VanNHdipi stress is most similar to responses to antibacterial agents inhibiting cell wall synthesis, such as vancomycin and lantibiotics.

Proteomic analysis. Comparative proteomics has proven useful to characterize the mode of action of compounds. The responses of *B. subtilis* to treatment with VanNHdipi or vancomycin were studied at the proteome level by combining 2D gel-electrophoresis and LC-MS analysis. Bacterial cultures at an OD_{500} of 0.35 were treated with either vancomycin or VanNHdipi at their respective PECs for 10 minutes. Subsequently, the newly synthesized proteins were pulse-labeled using L-(^{35}S)-methionine for 5 min and analyzed by 2D gel-electrophoresis and autoradiography. The resulting proteomic profiles revealed distinct signatures for vancomycin and VanNHdipi (Fig. 3B and C). Notably, some proteins were upregulated in response to both vancomycin and VanNHdipi, namely Hom, SdhA, NfrA, YtrB, YtreE, YpuA, and YceC, indicative of shared mechanisms of action (Table 1). YtrB and YtrE have previously been identified as marker proteins of an interference with membrane-bound steps of cell wall biosynthesis including bactoprenol recycling. Upregulation of these proteins is in line with VanNHdipi addressing the same target as vancomycin. However, 11 proteins were significantly upregulated upon treatment with VanNHdipi (**2**), but not upon treatment with vancomycin (Table 1). Crucially, proteins associated with general stress, cell envelope stress, and membrane stress, were strongly upregulated upon exposure to VanNHdipi, highlighting its distinctive impact on membrane dynamics. In particular, LiaH and PspA serve as markers of an impairment of the structural integrity of the cytoplasmic membrane. LiaH is specifically upregulated upon membrane stress, as opposed to peptidoglycan stress. It is also significantly upregulated upon treatment with daptomycin and lantibiotics.[32] Likewise, PspA is a marker for antibiotics interacting with the cytoplasmic membrane. It is upregulated upon envelope stress exerted by antibacterial agents such as daptomycin, gallidermin, nisin, valinomycin, gramicidin A, and gramicidin S, but not vancomycin or mersacidin, which are thought to not interact with membrane lipids.[33] Other proteins upregulated in response to VanNHdipi are involved in the reorganization of the membrane lipid composition such as FabL which is associated with fatty acid biosynthesis and YvcR, an uncharacterized membrane-bound ABC transporter ATP-binding protein.

Taken together, the proteome analysis indicates that the response to VanNHdipi shares hallmarks of the response to vancomycin, reflecting an interference with a membrane-bound step of cell wall biosynthesis. However, it also indicates that the mechanism of action is distinct from that of the parent drug, in that VanNHdipi interferes with the structural integrity of the membrane, like gallidermin, nisin and daptomycin (Fig. 3D and E).

Cell wall biosynthesis inhibition. To confirm the effects of VanNHdipi (**2**) on *B. subtilis* cell wall biosynthesis,

Table 1 Upregulation of proteins after treatment with vancomycin and VanNHdipi identified by radiolabeling newly synthesized proteins using a 2D gel-based approach

			Regulation factor	
Protein	Protein function	Biological process	Vancomycin/control	VanNHdipi/control
CysC	Probable adenylyl-sulfate kinase	Sulfate assimilation	2.3 ± 0.1	
FabL	Enoyl-[acyl-carrier-protein] reductase [NADPH]	Fatty acid elongation		41.9 ± 3.5[a]
GsaB	Glutamate-1-semialdehyde 2,1-aminomutase 2	Heme biosynthesis	2.8 ± 0.4	
Hom	Homoserine dehydrogenase	Amino acid metabolism	5.0 ± 3.8*	3.3 ± 1.0
KtrC	Ktr system potassium uptake protein C	Ion transport		5.4 ± 2.2
LiaH.1	LiaH	Cell envelope stress		67.3 ± 35.2
LiaH.2	LiaH	Cell envelope stress		131.3 ± 65.96
LiaH.3	LiaH	Cell envelope stress		45.7 ± 9.98
LysA	Diaminopimelate decarboxylase	Amino acid metabolism	2.7 ± 0.3	
MtnE	L-Glutamine-4-(methylsulfanyl)-2-oxobutanoate aminotransferase	Amino acid metabolism	2.4 ± 0.3	
MurF	UDP-*N*-acetylmuramoyl-tripeptide-D-alanyl-D-alanine ligase	Cell wall biosynthesis	4.1 ± 1.6	
NfrA	FMN reductase (NADPH)	Oxidative stress response	3.3 ± 0.2	2.7 ± 0.2
PspA	Phage shock protein A homolog	Cell envelope stress		8.2 ± 2.5
RpsB	30S ribosomal protein S2	Translation	2.7 ± 0.3	
RpsC	30S ribosomal protein S3	Translation		11.4 ± 12.7
SdhA	Succinate dehydrogenase flavoprotein	TCA cycle	3.3 ± 1	3.1 ± 0.9[a]
ThiG	Thiazole synthase	Cofactor biosynthesis	2.5 ± 0.1	
Udk	Uridine kinase	Nucleotide biosynthesis	3.1 ± 0.5	
YceC	Stress response protein SCP2	Cell envelope stress	3.7 ± 0.9	3.4 ± 1
YoxD	Uncharacterized oxidoreductase	Uncharacterized	2.9 ± 0.1	
YpuA	Uncharacterized protein	Cell envelope stress	4.4 ± 0.3	6.7 ± 1.95[a]
YqiG	Probable NADH-dependent flavin oxidoreductase	Uncharacterized	5.2 ± 1.3	
YtkL	UPF0173 metal-dependent hydrolase	General stress		5.7 ± 1.3
YtrB	ABC transporter ATP-binding protein	ABC transporter	4.8 ± 0.5	3.17 ± 0.4
YtrE.1	ABC transporter ATP-binding protein	ABC transporter		140.2 ± 40.5
YtrE.2	ABC transporter ATP-binding protein	ABC transporter	18.2 ± 8.98	13.55 ± 6.6[a]
YvcR	Uncharacterized ABC transporter ATP-binding protein	ABC transporter		± 5.5

[a] Indicates that protein was identified by inference rather than LC-MS.

a microscopy-based assay was performed. For this, the bacterial cells were cultured to an OD_{500} of 0.35 and then treated with compounds (vancomycin or VanNHdipi) at PEC for 10 minutes. Upon inhibition of a membrane-bound step in cell wall biosynthesis, new cell wall material is no longer incorporated into the cell wall.[34] This leads to a gradual weakening of the cell wall's structural integrity. When such compromised cells were subjected to a 1 : 3 mixture of acetic acid and methanol, bubbles appeared on the cell surface that show the membrane and cytoplasm blebbing out of these perforations. Bubble-like formations were observed on the bacterial cell surface upon treatment with both vancomycin and VanNHdipi (**2**) (Fig. 4A). These observations are consistent with both compounds inhibiting cell wall biosynthesis, compromising integrity of the cell wall, and resulting in structural vulnerabilities (Fig. 4A).

Membrane perturbation and delocalization of MinD protein. The proteomic response to VanNHdipi (**2**) indicated an interference with the structural integrity of the cytoplasmic membrane. To follow up on this, we first performed a MinD delocalization assay in *B. subtilis* (Fig. 4B). The maintenance of the transmembrane potential is crucial for the proper distribution and localization of cell division proteins like MinD.[35] In untreated, growing cells, MinD strongly localizes at the cell poles, and changes in its localization are often used as an

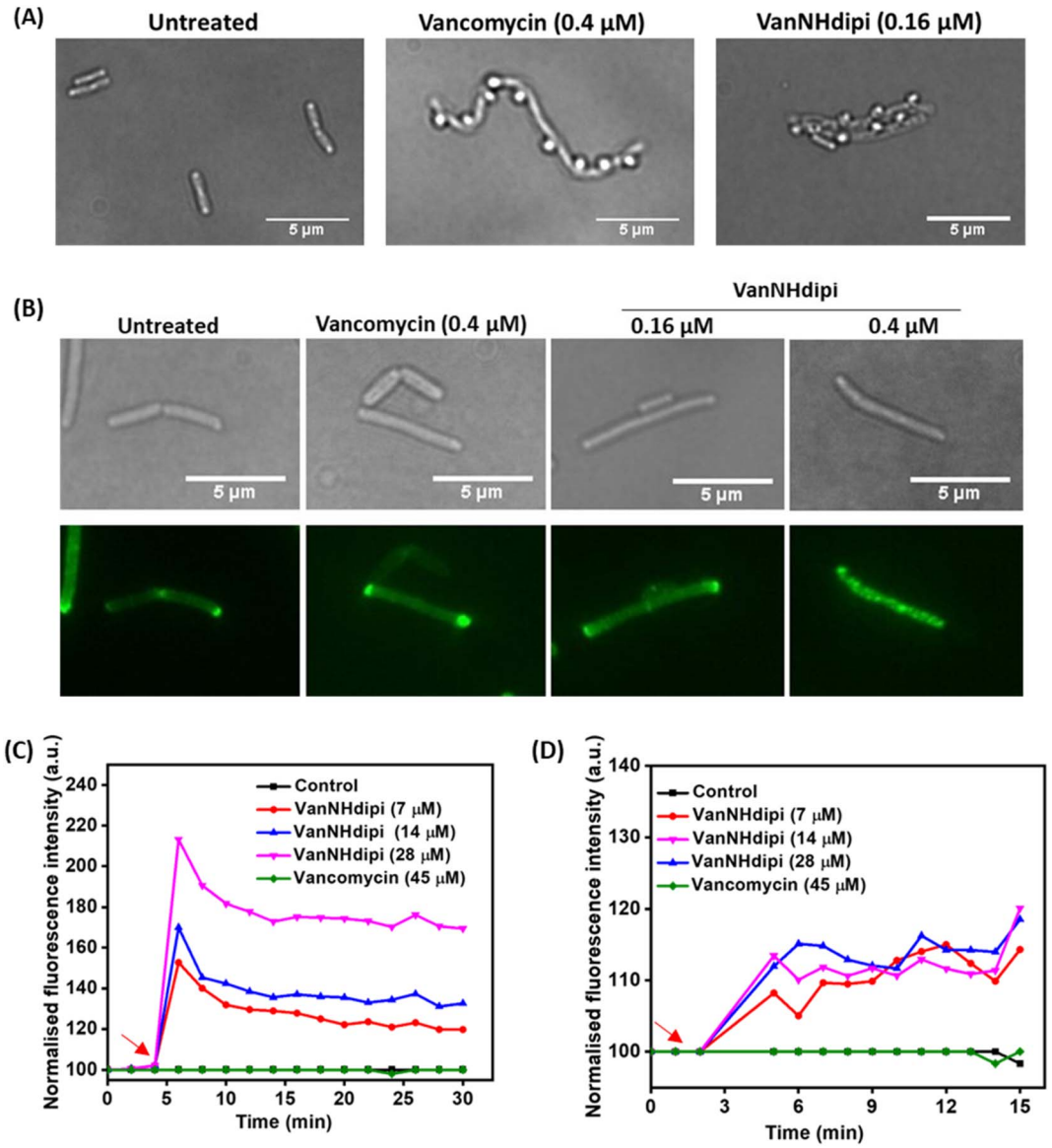

Fig. 4 Investigating the effect of vancomycin and VanNHdipi on the cell envelope. (A) Inhibition of cell wall biosynthesis in *B. subtilis* by vancomycin (0.4 μM) and VanNHdipi (0.16 μM) upon treatment at respective PECs, are indicated by bubble like structures on the surface of bacteria. (B) Delocalisation of the GFP-tagged MinD protein in *B. subtilis* by vancomycin at 0.4 μM (PEC) and VanNHdipi (**2**) at 0.16 μM (PEC) and 0.4 μM (MIC). Membrane (C) depolarisation and (D) permeabilization of exponential phase MRSA upon treatment with VanNHdipi (**2**); compound addition is indicated with red arrows. For the measurement of: depolarization, λ^{ex} 622 nm/λ^{em} 670 nm and for permeabilization, λ^{ex} 535 nm/λ^{em} 617 nm.

indicator of an impaired membrane potential and polarization. When the membrane potential is disturbed, MinD delocalizes, forming irregularly distributed spots throughout the cell.[35] In the assay, MinD localization is monitored by fluorescence microscopy using a GFP-MinD fusion protein. The microscopic studies were carried out by treating a GFP-MinD producing *B. subtilis* with vancomycin (at PEC = 0.4 μM) and VanNHdipi (at PEC = 0.16 μM and at 2 × MIC = 0.4 μM). As expected, vancomycin, which does not affect membrane integrity, did not elicit any MinD protein delocalization at its PEC (0.4 μM) which equals 2 × MIC.[31] It was found that VanNHdipi (**2**) did not induce delocalization of GFP-labelled MinD at the PEC (Fig. 4B). However, upon increasing the concentration to 0.4 μM (corresponding to MIC), ∼15% of the cells showed MinD delocalization (ESI S1†). This observation strongly implies that membrane perturbations induced by VanNHdipi become pronounced at a higher concentration. In summary, these results indicate that at 0.4 μM, VanNHdipi has a moderate effect on MinD localization, while vancomycin does not. The assay further indicates the impact of VanNHdipi on bacterial membrane dynamics.

A second set of assays was directed at investigating the impact of VanNHdipi (**2**) treatment on the bacterial membrane potential and its propensity to induce permeabilization in MRSA. Membrane depolarization was assessed by monitoring the fluorescence of the membrane potential-sensitive dye $DiSC_3(5)$ (3,3′-dipropylthiadicarbocyanine iodide), while permeabilization was monitored by the uptake of the propidium iodide dye (Fig. 4C and D). While vancomycin exhibited no discernible influence on the bacterial membrane even at 45 μM (approximately 55 × MIC), VanNHdipi demonstrated the capability to depolarize it at 7 μM (approximately 11.5 × MIC). This depolarization phenomenon exhibited a concentration-dependent pattern, becoming more pronounced with concentrations increasing up to 28 μM (Fig. 4C). Unlike membrane depolarization, which intensified with increasing compound concentration, membrane permeabilization remained relatively low and constant across a range of concentrations (Fig. 4D). Overall, the membrane integrity assays show that VanNHdipi, which through the incorporation of the benzyl-hexan-dipicolyl amine moiety to vancomycin has an additional hydrophobic element, possesses the potential to interact with bacterial membranes. In conclusion, the improved antibacterial activity of VanNHdipi results from a combination of inhibiting a membrane-bound step of cell wall synthesis and damage of membrane integrity.

VanNHdipi synergizes with carbapenems against Gram-negative bacteria

We previously reported that Dipi-Van (**1**) inhibits the NDM-1 enzyme and resensitizes NDM-producing Gram-negative bacteria to carbapenems.[28] Having validated the activity of VanNHdipi in Gram-positive bacteria, the applicability of the compound against Gram-negative bacteria was next investigated. The dipicolyl amine moiety is a known chelator of Zn(II) ion with a K_d of 160 nM.[36] Therefore, it was imperative to investigate the influence of the positional variation of dipicolyl amine in VanNHdipi (**2**) on the inhibition of metallo-β-lactamases, but also other effects attributable to metal chelation (Fig. S4†), such as a potential destabilization of the outer membrane.

VanNHdipi compromises the outer membrane integrity of Gram-negative bacteria. The outer membrane (OM) of Gram-negative bacteria serves as a permeability barrier and is vital to their intrinsic resistance to antibiotics like vancomycin.[37] The negatively charged outer membrane of the Gram-negative bacteria is stabilized by various divalent cations like Ca^{2+} and Mg^{2+}.[38] It was therefore hypothesized that the ability of dipicolyl amine to chelate the divalent cations, in conjunction with its hydrophobic characteristics, could potentially disrupt the integrity of the OM.[39] This disruption, in turn, may enhance permeability and allow the uptake of exogenous molecules. The kinetics of outer membrane permeabilization of VanNHdipi (**2**) were studied using the fluorescent probe, 1-*N*-phenylnaphthylamine (NPN). The outer membrane typically restricts the entry of hydrophobic substances like NPN, which can gain access to the hydrophobic phospholipid membrane upon permeabilization, resulting in fluorescence. However, upon treatment with VanNHdipi (**2**), the membrane of *K. pneumoniae* was found to undergo permeabilization, as evidenced by the higher fluorescence observed (Fig. S3†). This observation indicates the potential of VanNHdipi (**2**) to disrupt the outer membrane integrity of *K. pneumoniae R3934*, which could have significant implications for enhancing their susceptibility to VanNHdipi.

VanNHdipi resensitizes NDM-producing bacteria to carbapenems. The ability of VanNHdipi to permeabilize the membranes of Gram-negative bacteria suggests that the compound could access the periplasmic region where metallo-β-lactamases (MBLs) are located. VanNHdipi exhibited no inherent activity against Gram-negative bacteria, with MICs >50 μM for clinical isolates of *K. pneumoniae* R3934, BAA2146, EN5136 and *E. coli* EN5141. However, it had previously been reported that Dipi-Van (**1**) could resensitize NDM-1 producing pathogens to meropenem.[28] To investigate the ability of VanNHdipi to resensitize Gram-negative superbugs to carbapenems, checkerboard assays were performed (Table 2, Fig. 5, ESI S2†), testing combinations with meropenem and doripenem against various isolates of *K. pneumoniae* and *E. coli* expressing NDM enzymes. Among the tested strains, *K. pneumoniae* R3934 and BAA2146 expressed the NDM-1 enzyme,

Table 2 *In vitro* antibacterial activity of meropenem and doripenem in the presence of varying concentrations of VanNHdipi

	MIC (μg mL^{-1})					
	Meropenem + VanNHdipi (μg mL^{-1})			Doripenem + VanNHdipi (μg mL^{-1})		
Bacteria		16	32		16	32
K. pneumoniae EN5136	8	1	0.25	8	0.5	0.125
K. pneumoniae BAA2146	8	4	0.5	16	2	0.5
K. pneumoniae R3934	64	8	4	16	4	1
E. coli EN5141	2	0.13	0.06	8	0.5	0.25

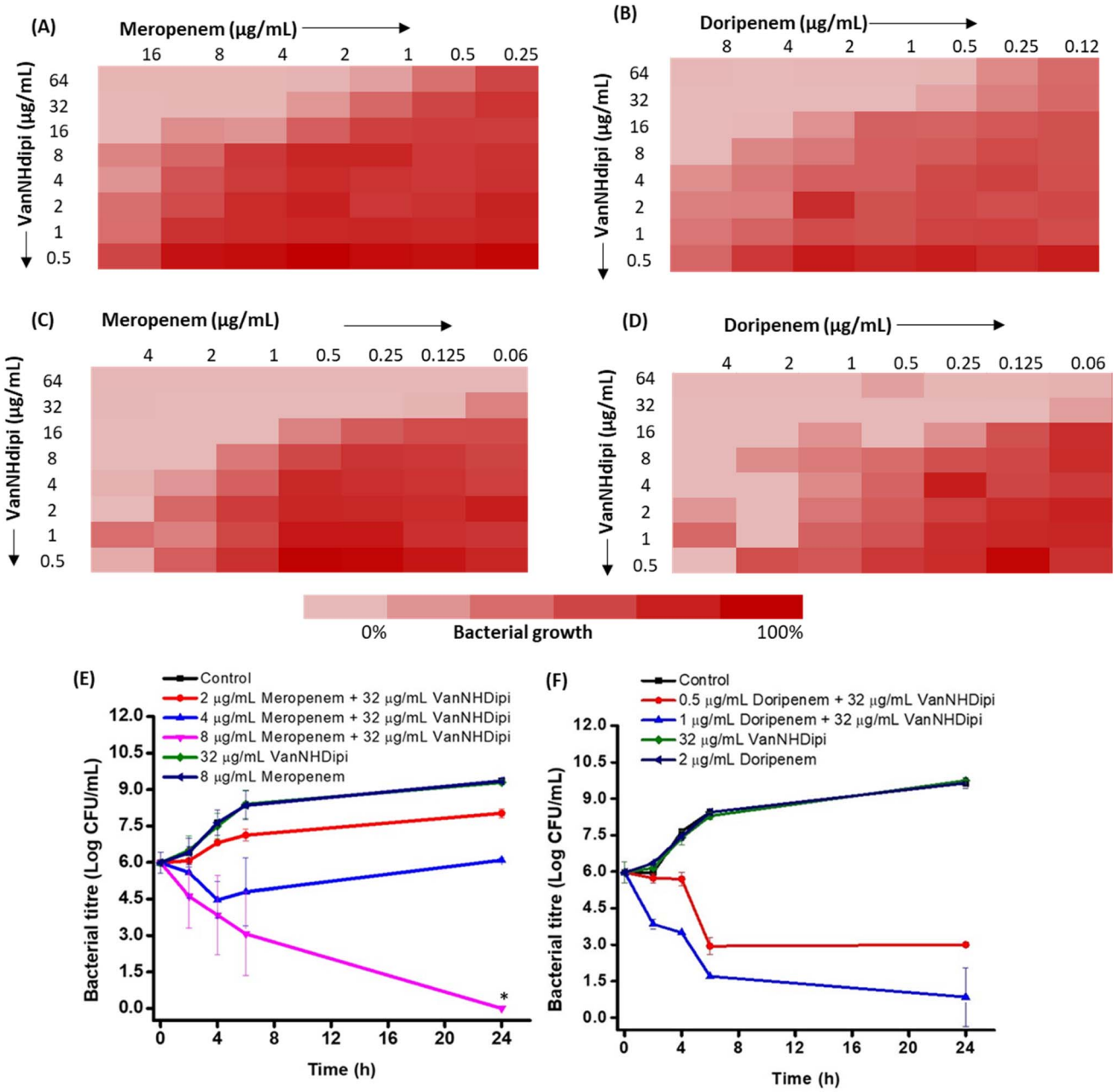

Fig. 5 VanNHdipi resensitizes NDM-producing bacteria to carbapenems. (A–D) Checkerboard assay to assess the effect of the combination of VanNHdipi (**2**) with meropenem and doripenem against NDM-1 positive *K. pneumoniae* R3934 (A & B) and *K. pneumoniae* EN5136 (C & D). Time-kill kinetics of (E) meropenem (F) doripenem in combination with VanNHdipi (**2**) against NDM-1 positive *K. pneumoniae* R3934. '*' indicates <50 CFU mL^{-1}. The lines for control, 8 μg mL^{-1} meropenem and 2 μg mL^{-1} doripenem perfectly overlap in E and F.

while *K. pneumoniae* EN5136 produced both the MBL NDM-1 and the serine-carbapenemase OXA-1, along with SHV β-lactamase enzymes. *E. coli* EN5141 produced the NDM-1 and OXA-1 β-lactamase enzymes. The OXA enzymes belong to class D β-lactamases, that can also hydrolyse carbapenems.[40]

We evaluated two structurally similar carbapenems, doripenem and meropenem (Fig. 5A–D). Doripenem is more active and undergoes slower hydrolysis by carbapenemases.[41] The clinical breakpoints of doripenem and meropenem against Gram-negative bacteria are 2 μg mL^{-1} and 1 μg mL^{-1}, respectively.[42] The MIC values of these carbapenems, against the clinical isolates tested ranged from 2 μg mL^{-1} to 64 μg mL^{-1} (Table 2). Susceptibility testing revealed that when exposed to 16 μg mL^{-1} of VanNHdipi (7 μM), NDM-1 expressing *K. pneumoniae* strains exhibited a 2-8-fold decrease in the MIC value of meropenem. Similarly, the MIC value of doripenem decreased by 4-16-fold for clinical isolates of NDM producing *K. pneumoniae* and *E. coli* in the presence of 16 μg mL^{-1} of VanNHdipi (7 μM) (Table 3). At a higher concentration of 32 μg mL^{-1} of VanNHdipi (14 μM), the MIC values of both meropenem and doripenem further reduced by 16–32-fold (MIC = 0.06–4 μg mL^{-1}) against all strains. However, the addition of an

Table 3 IC_{50} of Dipi-Van and VanNHdipi against various metallo-β-lactamases using absorbance (Abs)- and fluorescence (Fl)-based assays[a]

	IC_{50} (μM)			
MBLs	VanNHdipi (Abs)	VanNHdipi (Fl)	Dipi-Van (Abs)	Dipi-Van (Fl)
Class B1				
NDM-1	0.6 ± 0.1	0.2 ± 0.02	0.5 ± 0.1	0.4 ± 0.04
NDM-12	2.3 ± 0.6	0.6 ± 0.2	0.3 ± 0.06	0.1 ± 0.005
VIM-1	4.0 ± 0.4	3.6 ± 0.4	3.2 ± 0.6	1.9 ± 0.04
VIM-27	2.7 ± 0.4	5.0 ± 0.2	1.4 ± 0.04	3.5 ± 0.6
IMP-1	4.0 ± 1.7	1.2 ± 0.2	>40	>40
Class B2				
CphA	—	2.1 ± 1.1	—	>40
Class B3				
L1	11.0 ± 2.4	10.2 ± 2.8	7.2 ± 1.1	1.6 ± 0.3

[a] The fluorescence (Fl)-based assay measured for different MBLs is based on cleavage of chromophores CDC-1 and CPC-1.

equimolar amount of $ZnSO_4$ resulted in the loss of sensitization of *K. pneumoniae* to carbapenem (meropenem). This indicates that the inhibitory activity of VanNHdipi is associated with Zn(II) chelation (Fig. S5†). Overall, VanNHdipi demonstrated the ability to resensitize *K. pneumoniae* and *E. coli* strains expressing multiple β-lactamase enzymes to carbapenems.

Kinetics of bactericidal activity of combinations against NDM-producing pathogens. The ability of VanNHdipi to restore the bactericidal activity of carbapenems was studied by monitoring the kinetics of bactericidal activity against *K. pneumoniae* R3934 (KP R3934). Meropenem was ineffective against KP R3934 and did not show any growth inhibition upon treatment at 8 μg mL^{-1} alone (Fig. 5E). However, in the presence of 32 μg mL^{-1} of VanNHdipi (**2**), 4 μg mL^{-1} of meropenem maintained a static effect with bacterial titer of 6 Log CFU mL^{-1} against *K. pneumoniae* R3934. Increasing the concentration of meropenem to 8 μg mL^{-1} alongside 32 μg mL^{-1} of VanNHdipi (**2**) led to a significant decrease in bacterial count. Within 2 h, a reduction of 1.4 Log CFU mL^{-1} was achieved, which increased to 2.2 Log CFU mL^{-1} in 4 h, culminating in complete eradication in 24 h (6 Log CFU mL^{-1} reduction). Similarly, we tested the combination with doripenem. Doripenem alone, at 2 μg mL^{-1}, displayed no growth inhibition against KP R3934 (Fig. 5F). However, when combined with 32 μg mL^{-1} of VanNHdipi (**2**), a substantial reduction of the bacterial count was observed. At 0.5 μg mL^{-1} of doripenem in the presence of VanNHdipi, a reduction of 3 Log CFU mL^{-1} was attained within 6 h, which remained constant until 24 h. Upon increasing the doripenem concentration to 1 μg mL^{-1} in the presence of VanNHdipi (**2**), a substantial bacterial titer reduction occurred. Within 4 h, there was a decrease of 2.3 Log CFU mL^{-1}, which further accelerated to 4.2 Log CFU mL^{-1} within 6 h, ultimately achieving a 5 Log CFU mL^{-1} reduction after 24 h. This shows that treatment in combination with VanNHdipi potentiates and therefore restores the bactericidal activity of carbapenems.

Molecular docking and MD simulation studies of the interaction between VanNHdipi and NDM-1 enzyme. To substantiate our experimental results, we investigated the interaction between Dipi-Van and VanNHdipi with NDM-1 using molecular docking, followed by MD simulations. The molecular docking results showed that the dipicolylamine group in Dipi-Van and VanNHdipi interacts with the catalytic site residues of NDM-1. VanNHdipi (**2**) exhibited a binding energy (ΔG) of −8.7 kcal-mol^{-1}, whereas Dipi-Van (**1**) demonstrated a binding energy of −7.3 kcal mol^{-1}. Subsequently, we performed the 500 ns long MD simulations of the NDM-Dipi-Van and NDM-VanNHdipi docked complexes. Results revealed that the dipicolylamine group of both Dipi-Van and VanNHdipi interact within the active site of NDM-1. The vancomycin group of VanNHdipi is stably bound on the surface of NDM (Fig. 6A). In addition, we observed that the vancosamine sugar component of VanNHdipi interacts with the surface residues of NDM-1 through hydrogen bonding (Fig. 6B and S6†). Specifically, the sugar moiety in VanNHdipi (**2**) form H-bonds with Tyr64 and Arg45 residues of NDM-1 (Fig. S6† for more details). Moreover, the Arg52, Lys211, and Gly69 residues were also found to interact with the VanNHdipi (**2**) molecule, providing further stability to the complex (Fig. 6B). These H-bonding interactions could play a crucial role in stabilizing the alkyl chain connecting the vancosamine sugar to the dipicolylamine fragment. In Dipi-Van, stable H-bonding interactions were not observed due to the absence of the proximal sugar group, and the vancomycin group was flexible on the surface of NDM (ESI Fig. S7† for more details).

Importantly, the dipicolylamine fragment is in the vicinity of the active site of the NDM, which explains the deactivation of the NDM enzyme. In VanNHDipi, the stable vancomycin group stays on the surface of the protein, while the side chain compliments the contour of the protein surface and allows the dipicolylamine fragment to reach the active site (Fig. 6A). Dipicolylamine fragment likely forms a coordinated complex with Zn ions, thereby inhibiting NDM. However, as the MM force field we used is non-reactive, we could not see the formation of a covalent bond with Zn ions.

VanNHdipi exhibits inhibitory activity against various classes of metallo-β-lactamases. Building on our previous findings, finally, we wanted to test the inhibitory activity of these glycopeptide derivatives against various MBL enzymes.

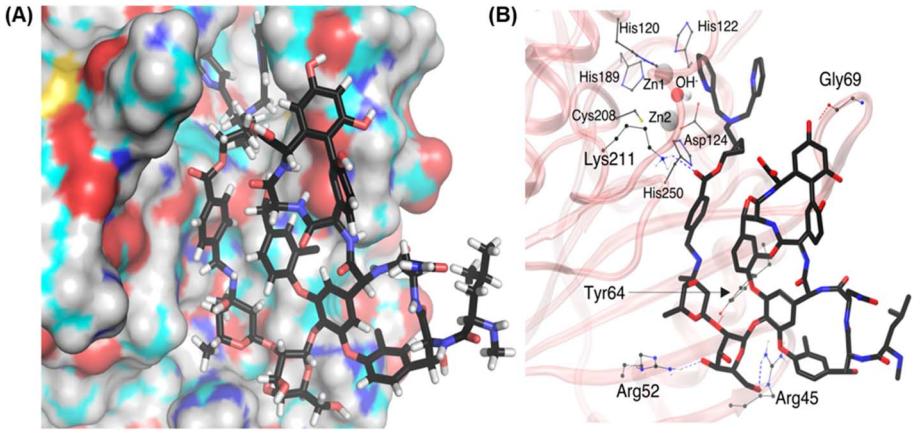

Fig. 6 Molecular docking and MD simulation study of VanNHdipi-mediated inhibition of NDM enzyme. (A) VanNHdipi (thick-stick representation) bound to the NDM-1 (surface representation) is shown. (B) The residues Tyr64, Arg45, Arg52, Lys211, and Gly69 are forming H-bonding interactions with VanNHdipi. Color code: C (black), O (red), N (blue), Zn (silver). Protein surface in (A) is color-coded by atom colors except that C is in cyan for clarity.

The MBLs are categorized into three subclasses-B1, B2, and B3 based on sequence and structural similarities and the number of Zn(II) ions in their active sites. Among these subclasses, the B1 enzymes, which include New Delhi metallo-β-lactamase(NDM), Verona-integron-borne metallo-β-lactamase (VIM), and imipenemase (IMP) families, are of particular clinical relevance.[43] They possess the ability to hydrolyze all β-lactam antibiotics, except aztreonam, and are not inhibited by any of the approved β-lactamase inhibitors.[43] The active sites of these enzymes contain zinc and are therefore inhibited by metal chelators, such as ethylenediaminetetraacetic acid *in vitro*.[44] Aspergillomarasmine A (AMA) has been recently reported as a potent inhibitor of the metallo-β-lactamases and also restores the activity of meropenem in MBL-producing Gram-negative bacteria.[45] Another example is a pyridine-2-carboxylic acid-based inhibitor, ANT431, that was designed to inhibit MBLs. The latter showed sub-micromolar inhibitory activity against NDM-1 and VIM-2 but was at least 20-fold less active against VIM-1 and IMP-1.[46] ANT431 demonstrated good potentiation of meropenem against Enterobacteriaceae that comprise NDM-1, but showed less potentiation against other MBL-producing variants.[46]

To explore the potential of Dipi-Van and VanNHdipi as broad-spectrum MBL inhibitors, we conducted *in vitro* tests on a panel of seven MBLs, representing each subclass. Two assays were employed: a nitrocefin-based absorbance assay and a fluorescence assay using chromophores CDC-1 and CPC-1.[47,48] These chromophores serve as substrates for MBL enzymes.[49] Hydrolysis of the β-lactam ring of nitrocefin by enzyme results in a shift in the ultraviolet absorption spectrum, allowing for visual detection of enzyme activity. On the other hand, CDC-1 and CPC-1 release a fluorescent probe, umbelliferone, upon hydrolysis, enabling quantification of enzyme activity.[50]

Class B1 MBLs are commonly associated with carbapenem resistance in human pathogens. These enzymes require one or two zinc ions at their active centers for full activity.[51] Dipi-Van showed an IC_{50} of 0.1–0.5 μM against NDM-1 and NDM-12. It also inhibited VIMs (VIM-1 and VIM-27) with an IC_{50} of 1.4–3.5 μM, albeit with reduced efficacy compared to NDM enzymes (Table 3, ESI S4 & S5†). However, Dipi-Van was inactive against the IMP-1 enzyme. On the other hand, VanNHdipi effectively inhibited all 5 class B1 enzymes tested including IMP-1 (S4 & S5†), with IC_{50} values ranging from 0.2–5 μM in both the absorbance and fluorescence assays with a 2-4-fold difference in IC_{50} values between the two assays (Table 3).

Class B2 enzymes contain one Zn(II) ion at their active site and specifically hydrolyse carbapenems.[52] Both compounds were tested against the CphA enzyme using the fluorescent probe CPC-1, which is a carbapenem-based probe.[47] Dipi-Van (**1**) did not inhibit CphA activity even at concentrations up to 40 μM, whereas VanNHdipi (**2**) showed an IC_{50} of 2.1 μM against this enzyme. Class B3 MBL enzymes are di-zinc enzymes with active-site architectures similar to B1 MBLs.[53] Against the Class B3 enzyme L1, both Dipi-Van and VanNHdipi demonstrated inhibitory activity, with IC_{50} values of 1.6–7.2 μM and 10.2–11 μM, respectively. It is important to note that the Zn(II)-chelating moiety, bis(pyridin-2-ylmethyl)amine (BPYA) alone, was found to inhibit enzyme activity with an IC_{50} of 1.2 μM against NDM-1 and 22.2 μM against VIM-27, while the IC_{50} against IMP-1 was greater than 40 μM (Fig. S8†). This indicates that there may be other factors contributing to the potency of VanNHdipi against IMP-1. The compounds were ineffective against the other β-lactamases, KPC-1 and AmpC, which are not MBLs (ESI S5†). Overall, we see that the two compounds differ in their spectrum of activity against MBLs. Although both derivatives share the same zinc binding moiety, they differ in their positioning on vancomycin and the linker. These differences in inhibitory activity suggest that the linker, orientation and steric factors imposed by the vancomycin core influence ligand access to the enzyme's active site. This is the first report of the use of glycopeptide analogues as inhibitors of a broad spectrum of MBLs. While this provides a promising starting point, the full potential of this application will require further systematic investigation in bacteria.

Conclusion

In this study, we introduced a dual-functional vancomycin derivative, VanNHdipi, that shows superior antibacterial activity over its predecessors. We not only demonstrate its enhanced activity against vancomycin-resistant bacteria, but also expand their application in resensitizing Gram-negative pathogens to last-line drugs, carbapenems. We emphasize that the position of modification of glycopeptide antibiotics significantly impact their biological activity and strategic modifications can be exploited to alter their efficacy. The vancosamine dipicolylamine vancomycin conjugate, VanNHdipi, shows superior activity against vancomycin-resistant Gram-positive bacteria as compared to the dipicolyl amine derivative functionalized at the C-terminus, Dipi-Van. VanNHdipi, also inhibits a broad spectrum of MBL enzymes while Dipi-Van, derivatized at the C-terminus, was limited in its activity. This leads the way for the design of molecules with better inhibitory activity against MBLs.

We provide insights into the mechanisms of action of new glycopeptide analogues against Gram-positive pathogens by exploring the mechanisms of VanNHdipi. In addition to vancomycin-like inhibition of cell wall biosynthesis, VanNHdipi acts through other mechanisms of action including disruption of structural integrity of the cytoplasmic membrane and inhibition of the membrane-bound stage of cell wall synthesis. The multifaceted mechanisms of action is advantageous over drugs with a single target, in that, they could slow the development of resistance.

Most importantly, we investigated the inhibitory activity of glycopeptide analogs against the various classes of MBL enzymes, an application that has not been explored previously. While our docking and MD simulation studies provide insights into the potential binding modes of Dipi-Van and VanNHdipi, further experimental approaches will be needed to fully understand mechanistic differences in MBL inhibition. With limited options available against MBL-producing Gram-negative pathogens, VanNHdipi presents a versatile alternative. Since examples of metal chelators used in the clinics are limited, the therapeutic potential of these vancomycin derivatives will need further rigorous assessment *in vivo* models. Overall, our research expands the scope of vancomycin derivatives presenting a promising new avenue for addressing antibiotic resistance.

Data availability

The datasets supporting this article have been uploaded as part of the ESI.† Data for the molecular dynamics simulation generated during the current study are not publicly available due to file size limitations but are available upon request.

Author contributions

P. S. conceptualized, designed, executed, and coordinated project; synthesized and characterized compounds, performed biological assays, curated and analyzed data, prepared original draft and revised manuscript. W. X., H. X. designed and performed metallo-ß-lactamase inhibition studies; S. T., N. N. N. performed molecular docking and molecular dynamics simulation studies; M. V. H., L. S., P. D. performed study of proteomic response of *B. subtilis;* J. E. B. supervised design and analysis of experiments for mechanistic studies in *B. subtilis;* D. B. synthesized and characterized compounds; G. D. performed *in vivo* activity against MRSA, checkerboard assays, and revised manuscript; J. H. conceptualized, supervised, coordinated research/manuscript writing, and acquired funding. All authors discussed the results and provided input to the manuscript.

Conflicts of interest

There are no conflicts of interest to declare.

Acknowledgements

We acknowledge DST-DAAD bilateral cooperation project (INT/FRG/DAAD/P-15/2018), DST-BRICS mutilateral cooperation project (DST/IMRD/BRICS/PilotCall2/MBLI/2018(G)) and JNCASR for funding. JEB acknowledges funding from the DAAD Program DST 2018 (57389759). We thank Dr Sidharth Chopra (Central Drug Research Institute, Lucknow) and Dr Sulagna Basu (National Institute of Cholera and Enteric Diseases, Kolkata) for the gift of drug-resistant clinical isolates.

References

1 H. M. Lee, J. Ren, K. M. Tran, B. M. Jeon, W. U. Park, H. Kim, K. E. Lee, Y. Oh, M. Choi, D. S. Kim and D. Na, *Commun. Biol.*, 2021, **4**, 205.
2 G. Meletis, *Ther. Adv. Infect. Dis.*, 2016, **3**, 15–21.
3 **https://www.ecdc.europa.eu**, 2022.
4 D. Zeng, D. Debabov, T. L. Hartsell, R. J. Cano, S. Adams, J. A. Schuyler, R. McMillan and J. L. Pace, *Cold Spring Harbor Perspect. Med.*, 2016, **6**, a026989.
5 J. A. Karlowsky, K. Nichol and G. G. Zhanel, *Clin. Infect. Dis.*, 2015, **61**, S58–S68.
6 M. T. Guskey and B. T. Tsuji, *Pharmacotherapy*, 2010, **30**, 80–94.
7 G. G. Zhanel, D. Calic, F. Schweizer, S. Zelenitsky, H. Adam, P. R. Lagace-Wiens, E. Rubinstein, A. S. Gin, D. J. Hoban and J. A. Karlowsky, *Drugs*, 2010, **70**, 859–886.
8 G. Dhanda, P. Sarkar, S. Samaddar and J. Haldar, *J. Med. Chem.*, 2019, **62**, 3184–3205.
9 M. A. T. Blaskovich, K. A. Hansford, Y. Gong, M. S. Butler, C. Muldoon, J. X. Huang, S. Ramu, A. B. Silva, M. Cheng, A. M. Kavanagh, Z. Ziora, R. Premraj, F. Lindahl, T. A. Bradford, J. C. Lee, T. Karoli, R. Pelingon, D. J. Edwards, M. Amado, A. G. Elliott, W. Phetsang, N. H. Daud, J. E. Deecke, H. E. Sidjabat, S. Ramaologa, J. Zuegg, J. R. Betley, A. P. G. Beevers, R. A. G. Smith, J. A. Roberts, D. L. Paterson and M. A. Cooper, *Nat. Commun.*, 2018, **9**, 22.
10 A. Antonoplis, X. Zang, M. A. Huttner, K. K. L. Chong, Y. B. Lee, J. Y. Co, M. R. Amieva, K. A. Kline, P. A. Wender and L. Cegelski, *J. Am. Chem. Soc.*, 2018, **140**, 16140–16151.

11 F. Umstatter, C. Domhan, T. Hertlein, K. Ohlsen, E. Muhlberg, C. Kleist, S. Zimmermann, B. Beijer, K. D. Klika, U. Haberkorn, W. Mier and P. Uhl, *Angew Chem. Int. Ed. Engl.*, 2020, **59**, 8823–8827.
12 D. Guan, F. Chen, Y. Qiu, B. Jiang, L. Gong, L. Lan and W. Huang, *Angew Chem. Int. Ed. Engl.*, 2019, **58**, 6678–6682.
13 M. B. Chosy, J. Sun, H. P. Rahn, X. Liu, J. Brcic, P. A. Wender and L. Cegelski, *ACS Infect. Dis.*, 2024, **10**, 384–397.
14 V. Yarlagadda, P. Sarkar, S. Samaddar and J. Haldar, *Angew Chem. Int. Ed. Engl.*, 2016, **55**, 7836–7840.
15 Y. Jiang, M. Han, Y. Bo, Y. Feng, W. Li, J. R. Wu, Z. Song, Z. Zhao, Z. Tan, Y. Chen, T. Xue, Z. Fu, S. H. Kuo, G. W. Lau, E. Luijten and J. Cheng, *ACS Cent. Sci.*, 2020, **6**, 2267–2276.
16 D. Guan, F. Chen, Faridoon, J. Liu, J. Li, L. Lan and W. Huang, *ChemMedChem*, 2018, **13**, 1644–1657.
17 A. Okano, N. A. Isley and D. L. Boger, *Proc. Natl. Acad. Sci. U. S. A.*, 2017, **114**, E5052–E5061.
18 Z. C. Wu, N. A. Isley and D. L. Boger, *ACS Infect. Dis.*, 2018, **4**, 1468–1474.
19 S. S. Printsevskaya, M. I. Reznikova, A. M. Korolev, G. B. Lapa, E. N. Olsufyeva, M. N. Preobrazhenskaya, J. J. Plattner and Y. K. Zhang, *Future Med. Chem.*, 2013, **5**, 641–652.
20 S. H. Werby, J. Brcic, M. B. Chosy, J. Sun, J. T. Rendell, L. F. Neville, P. A. Wender and L. Cegelski, *RSC Med. Chem.*, 2023, **14**, 1192–1198.
21 A. Antonoplis, X. Zang, T. Wegner, P. A. Wender and L. Cegelski, *ACS Chem. Biol.*, 2019, **14**, 2065–2070.
22 P. Sarkar, K. De, M. Modi, G. Dhanda, R. Priyadarshini, J. E. Bandow and J. Haldar, *Chem. Sci.*, 2023, **14**, 2386–2398.
23 Y. Acharya, S. Bhattacharyya, G. Dhanda and J. Haldar, *ACS Infect. Dis.*, 2022, **8**, 1–28.
24 E. van Groesen, P. Innocenti and N. I. Martin, *ACS Infect. Dis.*, 2022, **8**, 1381–1407.
25 V. Yarlagadda, G. B. Manjunath, P. Sarkar, P. Akkapeddi, K. Paramanandham, B. R. Shome, R. Ravikumar and J. Haldar, *ACS Infect. Dis.*, 2016, **2**, 132–139.
26 P. Sarkar, S. Samaddar, V. Ammanathan, V. Yarlagadda, C. Ghosh, M. Shukla, G. Kaul, R. Manjithaya, S. Chopra and J. Haldar, *ACS Chem. Biol.*, 2020, **15**, 884–889.
27 P. Sarkar, D. Basak, R. Mukherjee, J. E. Bandow and J. Haldar, *J. Med. Chem.*, 2021, **64**, 10185–10202.
28 V. Yarlagadda, P. Sarkar, S. Samaddar, G. B. Manjunath, S. D. Mitra, K. Paramanandham, B. R. Shome and J. Haldar, *ACS Infect. Dis.*, 2018, **4**, 1093–1101.
29 E. Banin, K. M. Brady and E. P. Greenberg, *Appl. Environ. Microbiol.*, 2006, **72**, 2064–2069.
30 D. G. Conrady, C. C. Brescia, K. Horii, A. A. Weiss, D. J. Hassett and A. B. Herr, *Proc. Natl. Acad. Sci. U. S. A.*, 2008, **105**, 19456–19461.
31 M. Wenzel, B. Kohl, D. Munch, N. Raatschen, H. B. Albada, L. Hamoen, N. Metzler-Nolte, H. G. Sahl and J. E. Bandow, *Antimicrob. Agents Chemother.*, 2012, **56**, 5749–5757.
32 A. Muller, M. Wenzel, H. Strahl, F. Grein, T. N. V. Saaki, B. Kohl, T. Siersma, J. E. Bandow, H. G. Sahl, T. Schneider and L. W. Hamoen, *Proc. Natl. Acad. Sci. U. S. A.*, 2016, **113**, E7077–E7086.
33 C. H. R. Senges, J. J. Stepanek, M. Wenzel, N. Raatschen, U. Ay, Y. Martens, P. Prochnow, M. Vazquez Hernandez, A. Yayci, B. Schubert, N. B. M. Janzing, H. L. Warmuth, M. Kozik, J. Bongard, J. N. Alumasa, B. Albada, M. Penkova, T. Lukezic, N. A. Sorto, N. Lorenz, R. G. Miller, B. Zhu, M. Benda, J. Stulke, S. Schakermann, L. I. Leichert, K. Scheinpflug, H. Brotz-Oesterhelt, C. Hertweck, J. T. Shaw, H. Petkovic, J. M. Brunel, K. C. Keiler, N. Metzler-Nolte and J. E. Bandow, *Antimicrob. Agents Chemother.*, 2020, **65**, e01373.
34 M. Wenzel, M. Patra, D. Albrecht, D. Y. Chen, K. C. Nicolaou, N. Metzler-Nolte and J. E. Bandow, *Antimicrob. Agents Chemother.*, 2011, **55**, 2590–2596.
35 H. Strahl and L. W. Hamoen, *Proc. Natl. Acad. Sci. U.S.A.*, 2010, **107**, 12281–12286.
36 B. A. Wong, S. Friedle and S. J. Lippard, *J. Am. Chem. Soc.*, 2009, **131**, 7142–7152.
37 K. L. May and M. Grabowicz, *Proc. Natl. Acad. Sci. U. S. A.*, 2018, **115**, 8852–8854.
38 L. A. Clifton, M. W. Skoda, A. P. Le Brun, F. Ciesielski, I. Kuzmenko, S. A. Holt and J. H. Lakey, *Langmuir*, 2015, **31**, 404–412.
39 E. R. Milaeva, D. B. Shpakovsky, Y. A. Gracheva, S. I. Orlova, V. V. Maduar, B. N. Tarasevich, N. N. Meleshonkova, L. G. Dubova and E. F. Shevtsova, *Dalton Trans.*, 2013, **42**, 6817–6828.
40 N. T. Antunes, T. L. Lamoureaux, M. Toth, N. K. Stewart, H. Frase and S. B. Vakulenko, *Antimicrob. Agents Chemother.*, 2014, **58**, 2119–2125.
41 A. M. Queenan, W. Shang, R. Flamm and K. Bush, *Antimicrob. Agents Chemother.*, 2010, **54**, 565–569.
42 **https://www.eucast.org**, 2021.
43 M. F. Mojica, R. A. Bonomo and W. Fast, *Curr. Drug Targets*, 2016, **17**, 1029–1050.
44 L. C. Ju, Z. Cheng, W. Fast, R. A. Bonomo and M. W. Crowder, *Trends Pharmacol. Sci.*, 2018, **39**, 635–647.
45 A. M. King, S. A. Reid-Yu, W. Wang, D. T. King, G. De Pascale, N. C. Strynadka, T. R. Walsh, B. K. Coombes and G. D. Wright, *Nature*, 2014, **510**, 503–506.
46 M. Everett, N. Sprynski, A. Coelho, J. Castandet, M. Bayet, J. Bougnon, C. Lozano, D. T. Davies, S. Leiris, M. Zalacain, I. Morrissey, S. Magnet, K. Holden, P. Warn, F. De Luca, J. D. Docquier and M. Lemonnier, *Antimicrob. Agents Chemother.*, 2018, **62**, e00074.
47 H. Xie, J. Mire, Y. Kong, M. Chang, H. A. Hassounah, C. N. Thornton, J. C. Sacchettini, J. D. Cirillo and J. Rao, *Nat. Chem.*, 2012, **4**, 802–809.
48 S. S. van Berkel, J. Brem, A. M. Rydzik, R. Salimraj, R. Cain, A. Verma, R. J. Owens, C. W. Fishwick, J. Spencer and C. J. Schofield, *J. Med. Chem.*, 2013, **56**, 6945–6953.
49 X. Qian, S. Zhang, S. Xue, W. Mao, M. Xu, W. Xu and H. Xie, *Bioorg. Med. Chem. Lett.*, 2019, **29**, 322–325.
50 W. Mao, L. Xia and H. Xie, *Angew Chem. Int. Ed. Engl.*, 2017, **56**, 4468–4472.

51 M. N. Lisa, A. R. Palacios, M. Aitha, M. M. Gonzalez, D. M. Moreno, M. W. Crowder, R. A. Bonomo, J. Spencer, D. L. Tierney, L. I. Llarrull and A. J. Vila, *Nat. Commun.*, 2017, **8**, 538.

52 M. Vanhove, M. Zakhem, B. Devreese, N. Franceschini, C. Anne, C. Bebrone, G. Amicosante, G. M. Rossolini, J. Van Beeumen, J. M. Frere and M. Galleni, *Cell. Mol. Life Sci.*, 2003, **60**, 2501–2509.

53 C. L. Tooke, P. Hinchliffe, E. C. Bragginton, C. K. Colenso, V. H. A. Hirvonen, Y. Takebayashi and J. Spencer, *J. Mol. Biol.*, 2019, **431**, 3472–3500.